THE KLOE ELECTROMAGNETIC CALORIMETER

JULIET LEE-FRANZINI

Laboratori Nazionali di Frascati
Via Enrico Fermi 40 - 00044 - Frascati, Italy
Physics Department, State University of New York at Stony Brook
Stony Brook, New York 11794, U.S.A.

and

A. ANTONELLI[b], M. ANTONELLI[b], G. BARBIELLINI[g], M. BARONE[b], S. BERTOLUCCI[b], C. BINI[d], C. BLOISE[b], V. BOLOGNESI[c], F. BOSSI[b], P. CAMPANA[b], F. CERVELLI[c], R. CALOI[d], M. CORDELLI[b], G. DE ZORZI[d], G. DI COSIMO[d], A. DI DOMENICO[d], O. ERRIQUEZ[a], A. FARILLA[a], A. FERRARI[c], P. FRANZINI[d], F. GARUFI[d], P. GAUZZI[d], E. GERO[b], S. GIOVANNELLA[b], R. HAYDAR[b], M. INCAGLI[c], L. KEEBLE[b], W. KIM[f], G. LANFRANCHI[b], A. MARTINI[b], A. MARTINIS[g], S. MISCETTI[b], F. MURTAS[b], A. PARRI[b], A. PASSERI[e], F. SCURI[g], E. SPIRITI[e], L. TORTORA[e], S.WÖLFLE[b].

[a] *Dipartimento di Fisica dell'Università e Sezione INFN Bari,*
[b] *Laboratori Nazionali di Frascati dell'INFN, Frascati,*
[c] *Dipartimento di Fisica dell'Università e Sezione INFN Pisa,*
[d] *Dipartimento di Fisica dell'Università e Sezione INFN Roma I,*
[e] *Istituto Superiore di Sanità and Sezione INFN, ISS, Roma,*
[f] *Physics Department, State University of New York at Stony Brook,*
[g] *Dipartimento di Fisica dell'Università e Sezione INFN Trieste/Udine.*

ABSTRACT

A general purpose detector, KLOE, is under construction for operations at the Frascati ϕ factory, DAΦNE. Its central mission is the study of direct CP violation in K^0 decays, which places very stringent requirements on electromagnetic shower measurements in the 20–280 MeV/c region. We have chosen to use a lead–scintillator sampling calorimeter, EmC, consisting of very thin (0.5 mm) lead layers in which are embedded 1 mm diameter scintillating fibers. Much prototyping and testing has been done during its design, yielding, for the final EmC, an expected energy resolution of $\sigma(E)/E \sim 5\%/\sqrt{E\ (\mathrm{GeV})}$ and a time resolution of $\sim$66 ps$/\sqrt{E\ (\mathrm{GeV})}$, with excellent linearity in the region of interest and with little dependence on incidence angle and entry position.

1. Introduction

The main goal of the KLOE[1] experiment at the DAΦNE ϕ-factory[2] in Frascati is to study CP violation in K^0 decays by measuring $\Re(\epsilon'/\epsilon)$ with an accuracy of $\mathcal{O}(10^{-4})$. Since $K_{L,S}$ neutral decays ($K_{L,S}\to\pi^0\pi^0$) produce four photons between 20 and 280 MeV, identification of these decays and rejection of the $K_L\to3\pi^0$ background[1] means that the electromagnetic calorimeter (EmC) plays a crucial role in this measurement. Vertex reconstruction of $K^0\to\pi^0$'s$\to\gamma$'s in KLOE is performed by measuring the arrival time of each photon the the calorimeter ;[3] because of the low speed of the K^0 ($\beta_K\sim0.2$), requiring excellent timing accuracy of the EmC. In addition, the calorimeter should also provide a fast and unbiased first level trigger for the detector. Finally, it should have some particle identification capability, to aid rejection of $K_{\mu3}$ decays. The requirements for the KLOE EmC are: a) time resolution $\mathcal{O}(70\text{ ps}/\sqrt{E\text{ (GeV)}})$, b) energy resolution $\mathcal{O}(5\%/\sqrt{E\text{ (GeV)}})$, c) shower vertex resolution $\mathcal{O}(1\text{ cm})$, d) full efficiency for γ's in the energy range 20–280 MeV, and e) hermeticity.

2. The KLOE Electromagnetic Calorimeter Design

The KLOE EmC is a very fine sampling lead-scintillating fiber calorimeter, with photomultipliers, PMs, read-out. The central part, barrel, approximates a cylindrical shell of 4 m inner diameter, 4.3 m active length and 23 cm thicknes. The barrel covers the polar angle region $49°<\theta<131°$and consists of 24 sectors with trapezoidal cross section, ~60 cm wide. Two end-caps, 4 m in diameter and 23 cm thick, close hermetically the calorimeter. Each end-cap, consists of 26 "C" shaped modules which run vertically along the chords of the circle inscribed in the barrel. At the two ends they are bent at 90°, becoming parallel to the barrel ends, to decrease the effects of the magnetic field on the PMs and to increase hermeticity. A quater cross section of the KLOE calorimeter is shown in fig. 1. In our EmC fibers run mostly transversely to the particle trajectories. This reduces sampling fluctuations due to channeling, resulting in improved resolution particularly important at low energies.

Each module of the KLOE EmC is built by glueing 1 mm diameter blue scintillating fibers between thin grooved lead plates, obtained by passing 0.5 mm thick lead foils through rollers of proper shape. The grooves in the two sides of the lead are displaced by one half of the pitch so that fibers are located at the corners of adjacent, quasi-equilateral triangles resulting in optimal uniformity of the final stack, see fig. 2. The grooves are just big enough to insure that the lead does not apply direct pressure on the fibers. Light travelling in the cladding is effectively removed because of the glue surrounding the fibers. The selected fiber pitch of 1.35 mm results in a structure which has a fiber:lead:glue volume ratio of 48:42:10 and a sampling fraction of ~15% for a minimum ionizing particle. The final composite has a density of ~5 g/cm^3 and a radiation length X_0 of ~1.6 cm, is self supporting and can be easily machined. The very small lead foil thickness ($< 0.1\,X_0$) results in a quasi–homogeneous structure and

in high efficiency for low energy photons. Measurements indicate that the blue-green Kuraray SCSF-81, Bicron BCF-12 and Pol.Hi.Tech-46 fibers, satisfy our requirements for light yield, scintillation decay time and attenuation length.[4] Since the time resolution depends on the light yield, great care has been put in maximizing the efficiency of the light collection system and insuring uniform photocathode illumination. Each light guide consists of a mixing part and a Winston cone concentrator.[5] We are thus able to match the calorimeter elements to the PM photocathodes, with an area reduction factor of up to ~4, without losses, because of the small divergence angle, 22°, of the light travelling in the fibers.

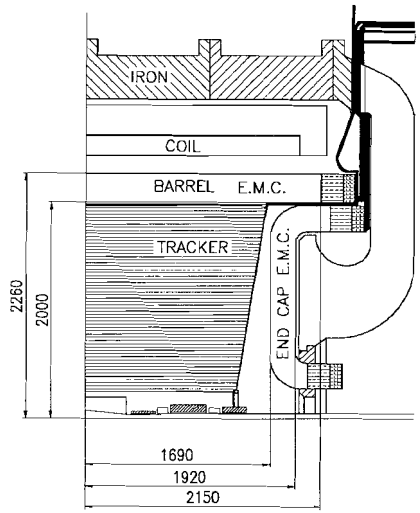

Fig. 1. Cross section of the KLOE Calorimeter

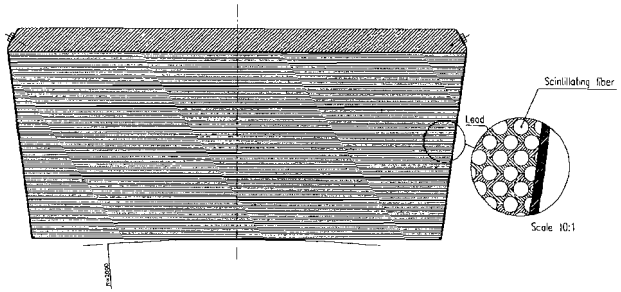

Fig. 2. Fiber and lead layout.

3. Construction of Prototypes

We built a *barrel* prototype module of dimensions $14\times24\times203$ cm^3 to establish construction procedures and perform realistic tests of the final EmC performance, see fig. 3a). The module depth of 24 cm is equivalent to a thickness of 15 X_0, consisting of 207 lead and scintillating fiber layers for a total of 21,450 fibers, the first 3.5 cm are Kuraray SCSF-81 fibers followed by 20.5 cm of Kuraray SCSF-38 fibers. It weighs 330 kg. The module was made in the Frascati machine shop. The grooved lead foils were produced with a home-made rolling machine starting from 0.5 mm thick lead foils. The grooved rollers, made of hardened steel and ground to shape by a sintered diamond tool, are mounted with ball bearings on a very rigid frame and are aligned and checked with a set of micrometers. Foils of almost 6 m length and 15 cm wide have been produced. The thickness uniformity obtained is around few tens of μm, the grooves deviate from a straight line by less than 0.1 mm per meter of foil length. The module was constructed by glueing the first lead foil to a 2 cm thick iron back plate carrying all the mounting fixtures. Bicron optical epoxy resin, BC 600 ml, was then applied in a precisely measured amount to the top surface of each lead foil. A layer of fibers was then laid down in the grooves and epoxy applied anew. Typically, 6–7 layers of fibers and lead were stacked in about one hour, before the glue started curing. The growing stack was then compressed under vacuum for at least 30 min to apply uniform pressure, and to squeeze out excess glue. Once the final thickness was reached the two ends were cut and milled. No fiber was damaged during the stacking phase, while four fibers were lost during the final milling. The calorimeter was wrapped in a 1 mm thick steel skin, in order to simulate the final design and provide protection for the module.

A prototype for the *end-cap* region, fig. 3b), consisting of two "C" shaped modules, was also built. The width of each module is 7 cm and they both have the same depth of 24 cm. Each section consists of a central straight piece (89–110 cm), two curved pieces with an inner radius of 7.5 cm, and two straight end pieces to which light guides are glued, the first 7 cm are Kuraray SCSF-81 fibers, the rest are Pol.Hi.Tech-46 fibers. It has been constructed by cutting the grooved lead foils and fibers to the desired lengths, incising at the two ends the central groove of each lead foil, leaving the central part uncut for a length of 89 cm, then bending the two adjacent modules.

The readout, identically for both prototypes, was organized into 22 elements for each side: five planes of four small elements, 3.5×3.5 cm^2, and two large rear elements, 6.5×7 cm^2, see fig. 3b). For the small elements, on each side the light was transported from the calorimeter through light guides to 1-1/8 inch diameter PMs, with an area concentration factor of $\sim$2.7. 1-1/8 inch Hamamatsu phototubes, type R1398 with a transit time spread of ($<$ 1 ns) have been used. The rear elements were similarly coupled to 5 cm diameter PMs, with an area concentration factor of $\sim$2.5.

In order to investigate the effect of coarsening the readout granularity and using larger light guides, we took data with the *barrel* readout organized in four planes of three 4.2×4.2 cm^2 cells, leaving the last plane unchanged. This configuration is referred to as "coarse" granularity, see fig. 3a). Since the same PMs were used, the light guides had an area concentration factor of $\sim$3.8.

4. Prototype Tests

4.1 Test Beams Layout

The calorimeter prototypes have been tested[6,7] in a beam at the Paul Scherrer Institut, PSI, in Villigen, Switzerland. The PSI machine is an isochronous cyclotron which accelerates protons to 600 MeV kinetic energy. A secondary beam of π's, μ's and e's in the momentum range 50–400 MeV/c was delivered to the test areas.

Two crossed scintillators in front of the calorimeter and a third counter, 4.5 m away from the calorimeter, provided a beam trigger, defined the beam position at the calorimeter and enabled $\pi/\mu/e$ identification by time of flight, see fig. 4.

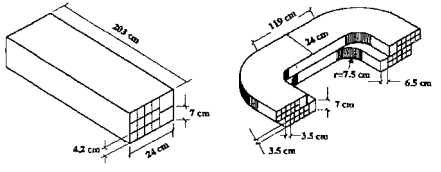

Fig. 3. a) *Barrel* and b) *end-cap*prototype.

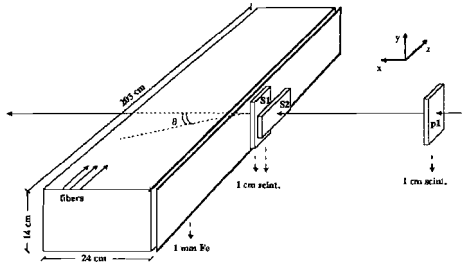

Fig. 4. Calorimeter test setup at PSI.

The calorimeter PM outputs were connected to active splitters through 5 m of RG-58 cable. The two outputs of each splitter were sent to CAMAC ADCs, to low threshold (5 mV) discriminators, the signal for 50 MeV being $\sim$350 mV. The discriminator outputs acted as TDC stops. The trigger signal was used to generate the ADC gates and the reference time signal T_0 which supplied the "start" for the TDC system.

The *barrel* prototype has also been tested with tagged low energy photons (20–80 MeV) at the Frascati LADON facility.[8] At LADON photons are obtained by

back scattering a laser beam from electrons stored in ADONE. A tagging system for the recoil electrons yields a determination of the photon energy with a resolution of ~1.7 MeV. The trigger was obtained by a coincidence from the two calorimeter ends, after adding all signals from each side. The trigger generated ADC gates and TDC "start"s which were cleared if there was no trigger from the tagging system within 200 ns.

4.2 Energy Response and Resolution

The coordinate system used in the data analysis is shown in fig. 4, where the definition of the incidence angle θ is also indicated. The origin was put in the center of the calorimeter surface facing the beam.

In order to study the energy response of the prototype we define the total visible energy E_{vis} as the sum over all elements read out on both ends, labelled A and B. To correct for the response of each channel we divided the signal $E_{adc,i}$ of channel i, by the calibration constants $K_{mip,i}$: $E_{vis} = (1/2)\sum(E_{A,i} + E_{B,i})$ with $E_i = E_{adc,i}/K_{mip,i}$. The calibration constants K_{mip}, in ADC counts, were obtained with cosmic rays and 400 MeV/c pions, both of which are minimum ionizing particles to a first approximation, incident at the center of each element. Clean samples of events selected for the calibration were ensured by means of triggering and software cuts. A gaussian fit to the pulse height distribution was performed for each channel to determine the peak position. The fit interval was chosen to be asymmetric with respect to the mean value, to take into account the asymmetric shape of the distribution.

We define 1 MIP as the visible energy deposited by a minimum ionizing particle in a 3.5×3.5 cm^2 readout element; our simulation[9] determines 1 MIP to be equivalent to an average energy deposit of 3.24 MeV in the active material. For the coarse granularity and for the larger cells of the last plane geometrical correction factors have been used to express the results in our calibration units. Pions of 400 MeV/c momentum are minimum ionizing particles only in the first plane of the calorimeter. We have therefore corrected for the increase of the specific ionization with calorimeter depth and for straggling effects. The correction factors used for both granularities are given in table 1.

Table 1. Specific ionization correction factors.

Plane Number	1	2	3	4	5	6
3.5 × 3.5	1.00	1.03	1.04	1.06	1.10	1.14
4.2 × 4.2	1.01	1.04	1.05	1.09	1.14	–

Before reaching the calorimeter the beam had to pass through the trigger counters and the iron skin of the calorimeter itself. The total amount of material is equivalent to 3.6 cm of scintillator. Positrons lose ~7 MeV while the energy loss of pions and muons depends on their kinetic energy and was appropriately taken into account.

These corrections have been applied to the beam energy of the charged particles.

Energy Response and Resolution for Photons and Positrons

The following results were obtained with positrons and photons entering the center of the calorimeter front face ($z = 0$ cm, $\theta = 0°$). The distributions of the energy signal for photons ranging from 28 to 63 MeV are are displayed in fig. 5. From the very good symmetry of the line shape at the lowest energy of 28 MeV, we can conclude that at these energies, the calorimeter is still fully efficient.

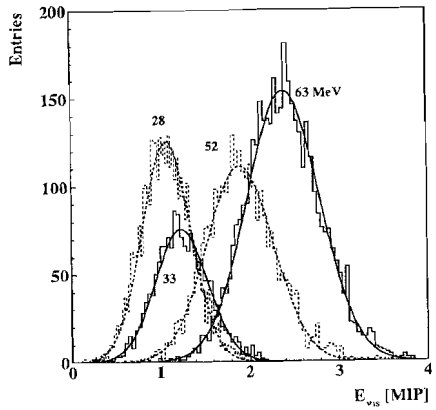

Fig. 5. Energy spectra for photons.

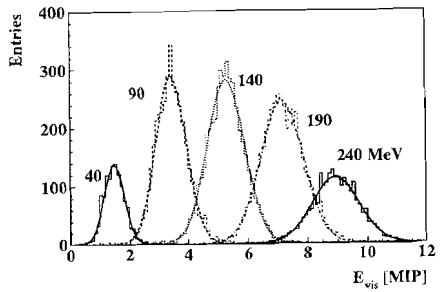

Fig. 6. Energy spectra for positrons.

For each spectrum a gaussian fit, leaving all three parameters free, has been performed; the mean of the fit was used as the average calorimeter response E_{vis} and the square root of the variance $\sigma_{E,vis}$ was used to compute the energy resolution. The plot of E_{vis}/E *vs.* the energy E have a maximum deviation from linearity of less than 3%, mostlty due to inaccuracies in tagging system. The line shapes for positrons

in the energy range 40–240 MeV are shown in fig. 6 for *barrel* data with the coarse granularity. The linearity of the response is excellent with a deviation of at most 2%, again mostly from beam setting inaccuracies.

Fitting photon and positron data together we obtain a slope $s_{barr} = (36.8 \pm 0.2)$ MIP/GeV, see fig. 7. In the same plot we have also added data for the *end-cap* prototype exposed to positrons (triangle symbols) for which the slope is $s_{ecap} = (37.4 \pm 0.6)$ MIP/GeV. The average response to electromagnetic (e.m.) showers is proportional to the incident particle kinetic energy only if the shower is fully contained. Simulations[9] show that the depth of the prototype keeps leakage below the 2% level for the energy range of interest. The sampling fraction for e.m. showers can therefore be estimated as $f_{em} = E_{vis}/E = (36.8 \pm 0.2)$ MIP/GeV $\times$ 3.24 MeV/MIP $= (11.9 \pm 0.1)\%$.

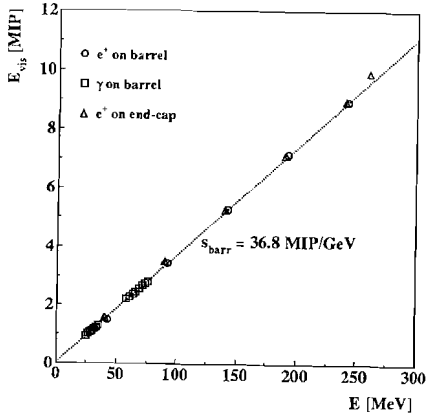

Fig. 7. Energy response for photons and positrons vs. kinetic energy.

The fluctuation of the ratio R between the energy signals, from each readout element, E_A and E_B at the two calorimeter ends, $R = E_A/E_B$, allows us to estimate the number of photoelectrons N_{pe} in each tube, from $N_{pe} = (\sqrt{2} \times \mu_R/\sigma_R)^2$, where μ_R and σ_R are the mean of R and the r.m.s. spread of its distribution respectively. For the *barrel* prototype the typical signal for a minimum ionizing particle at 1 m distance from the photomultiplier is ~65 pe. Results within 10% were obtained by measuring the PM gain directly. A lower light yield of ~50 pe/MIP is obtained in the *end-cap* prototype due to the worse quality fiber used in its construction. y resolution for positrons is $\sigma_E/E = (4.47 \pm 0.02)\%/\sqrt{E\ (\mathrm{GeV})}$ and for photons $\sigma_E/ = (4.35 \pm 0.01)\%/\sqrt{E\ (\mathrm{GeV})}$. The measured resolution for positrons and γ's are shown in fig. 8. The $1/\sqrt{E}$ dependence indicates that sampling fluctuations and photoelectron statistics dominate the resolution. The contribution of the latter has been evaluated from the light yield to be $1.6\%/\sqrt{E}$ and is therefore negligible. A similar analysis for the *end-cap* gives an energy resolution of $\sigma_E/E = (4.59 \pm 0.04)\%/\sqrt{E(\mathrm{GeV})}$.

Energy Response and Resolution for Pions and Muons

The response for muons and pions in the momentum range 150–280 MeV/c, of interest for the KLOE experiment, has also been studied. Due to their low kinetic energy (50–180 MeV) these particles lose energy mostly by ionization and could stop in the calorimeter. The response *vs.* kinetic energy for both types of particles is identical. A linear fit of the energy response curve gives a slope s_μ 46.8 MIP/GeV, corresponding to a sampling fraction for muons of $f_\mu = E_{vis}/E =$ 46.8±0.4 MIP/GeV×3.24 MeV/MIP = 15.2±0.1% and an "e/μ" ratio of f_e/f_μ=0.79. The energy resolution does not scale perfectly with $1/\sqrt{E}$ because sampling fluctuations become larger near the end of the particle's range. However, an approximate parametrization of the resolution is given by $3.7\%/\sqrt{E}$.

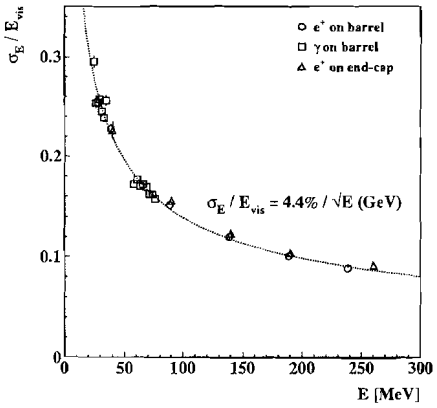

Fig. 8. Energy resolution for photons and positrons vs. kinetic energy.

Dependence on the z–coordinate

A z–scan along the module axis was performed with 200 MeV/c positrons at seven different z–positions from −80 to +80 cm. The z dependence of the signal is well represented as $E_{vis}(z) = E_{vis}(0)\cosh(z/\lambda)$, due to adding two exponentials, with an attenuation length λ=240 cm, while the resolution is constant.

Dependence on the Incidence Angle

The response of the barrel prototype as a function of the incidence angle, θ, has been studied using photons, positrons and muons at 30°, 45° and 60° incidence. Response and resolution do not depend on θ as expected for a quasi homogeneous calorimeter with very thin converter layers. For low energy photons. E <60 MeV, we observe a small worsening of the resolution, ~25%, at θ = 60°. The curved parts of the end-cap prototype have been investigated by scanning the prototype with 200 MeV positrons incident at 45° at different positions, moving along the outer surface of the bent part. No appreciable variation was found in the scan.

4.3 Timing Performances

The particle arrival time in the calorimeter is given, for each PM, by a discriminator output, used as a TDC "stop". For charged particles, the common "start" of the TDC system was obtained from the beam defining counters. For photons we self triggered on the analog sum of all calorimeter signals, as mentioned previously. Time walk correction depending on pulse height were applied off–line. The times measured at each calorimeter end T_A, T_B are obtained by the energy weighted average over all elements: $T_A = \sum E_{A,i} T_{A,i} / \sum E_{A,i}$; $T_B = \sum E_{B,i} T_{B,i} / \sum E_{B_i}$. The average of T_A and T_B then defines the mean arrival time T. For photons we perform our analysis in terms of the time difference $\Delta T = (1/2) \sum E_i (T_{A,i} - T_{B,i}) / \sum E_i$, ΔT and T are the difference and sum of T_A and T_B and therefore have the same r.m.s. spreads, *i.e.* $\sigma_{\Delta T} = \sigma_T$ except for the fact that the "start" time jitter is cancelled event by event in ΔT while it has to be unfolded for the external trigger case.

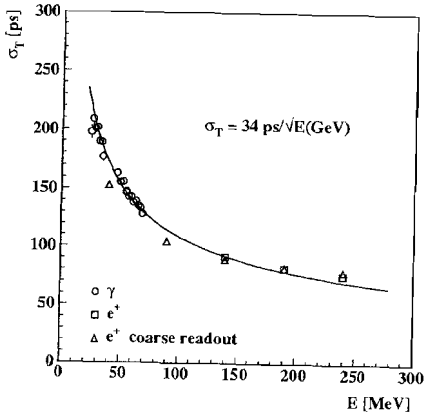

Fig. 9. Time resolution vs. energy.

Timing Resolution at Normal Incidence

The dependence of $\sigma_{\Delta T}$ on beam energy for 20–80 MeV γ's and of σ_T for 50–250 MeV positrons, at normal incidence on the calorimeter surface, are shown together in fig. 9, corresponding to a time resolution of $\sigma(T \text{ or } \Delta T)$=34 ps/$\sqrt{E\ (\text{GeV})}$. Fitting all measurements of $\sigma_{\Delta T}$ from 20 to 250 MeV gives $\sigma_{\Delta T}$=36 ps/$\sqrt{E\ (\text{GeV})}$, in excellent agreement with the result requiring unfolding of the "start" uncertainty. The measurements of the time resolution with a coarser readout granularity, (4.2×4.2 instead of 3.5×3.5 cm^2) triangle symbols in fig. 9, are indistinguishable although the light guides area reduction factor increases from 2.7 to 3.8, showing that light collection efficiency is unchanged. For the end-cap prototype we find a time resolution of σ_T =40 ps/$\sqrt{\text{E(GeV)}}$, with 50–200 MeV positrons.

Timing Resolution Dependence on Incidence Angle

The dependence of σ_T on θ was studied for all available beam energies. At 60° the resolution for 250 MeV positrons is ~25% worse than the result for normal incidence. The distributions are still gaussian. At lower energies the angular dependence of the resolution becomes negligible, being dominated by sampling fluctuations. The investigation of the curved portion of the end-cap prototype as described, found no dependence. Only for the most extreme conditions, when the shower effectively crosses the fibers twice, the time resolution deteriorates by ~20%.

Timing Resolution Dependence on z-Coordinate

All our measurements confirm that the time resolution scales as the number of photons to the $-1/2$ power. We therefore expect that the resolution is best at the center of the calorimeter. The z dependence of the time resolution is given by: $\sigma_T(z) = \sigma_T(0)\sqrt{\cosh(z/\lambda)}$. This has been verified with the data from the z–scan. The resolution at the two ends of the barrel module is ~1.05 times worse than at the center.

Measurement of the z–Coordinate

The z–coordinate of the entry point z_e obtained from the time difference ΔT and the effective light propagation speed in the fibers v_f is: $z_e = v_f \Delta T$. ΔT is plotted *vs.* the nominal z–position in fig. 10. From a fit to the data we obtain v_f=17.2 cm/ns, in agreement with the refractive index of the fiber core, n=1.6, and the bounce angle in the fiber.

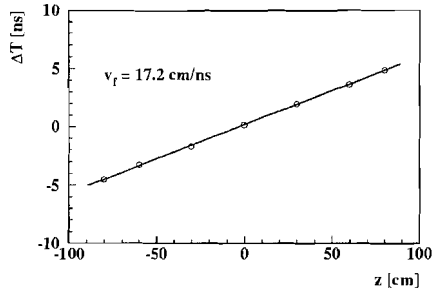

Fig. 10. ΔT distribution vs. nominal z-position for 200 MeV positrons.

The position resolution σ_z, given by $\sigma_z = v_f \sigma_{\Delta T}$ is σ_z=6 mm/$\sqrt{E\ (\text{GeV})}$ for the e.m. showers.

5. Particle Identification

$K_L \to \pi\mu\nu$ decay, $K_{\mu 3}$, constitutes the most significant background to the identification of $K_L \to \pi^+\pi^-$ decays. The calorimeter can provide some π/μ identification to improve the background rejection from kinematics.[10] π/μ identification can be

obtained by time of flight, Monte Carlo studies[3] show that the time resolution of the KLOE calorimeter, combined with tracking information result in a $K_{\mu 3}$ rejection factors of 5–6, with 93% signal efficiency. π/μ identification can also be achieved by studying the energy signals and the first and second moments of the energy deposition distributions in the calorimeter. This method has been tested with data collected for pions and muons of 200–250 MeV/c, a $K_{\mu 3}$ rejection factor of 5 for is obtained while maintaining an efficiency of 95% for pions.

6. Module Ø

All the machinery for building the *barrel* calorimeter have designed and built by the KLOE calorimeter group, mostly at the Laboratori Nazionali di Frascati, LNF. The first full size *barrel* module, with dimensions of 23 cm×60 cm×430 cm and trapezoidal cross section, called module Ø, was then succesfully built, also at Frascati. The machinery has been turned over to a company which will assemble all modules of the *barrel* calorimeter. The front half of module Ø is built with Kuraray SCSF-81 fibers and the back half with Pol.Hi.Tech-46 fibers.

The module read out consists of five planes of 12 elements each, of ~4.4×4.4 cm^2, varying slowly across the module face. Each element is viewed through light pipes which provide mixing and terminate with a Winston concentrator coupled to mesh photomultipliers. The PMs are manufactured to KLOE specifications by Hamamatsu (R2021, mod.). KLOE needs to use these special tubes because they can operate in moderate magnetic field.[11] As shown in fig. 1, they are inside the return yoke where they see up 0.15 T inclined less than 25° with respect to the PM's axis.[12] These PMs have a measured quantum efficiency ~60% lower than conventional tubes like the ones used in the previous prototypes.[13]

Module Ø employs the final KLOE electronics. The PM base contains the voltage divider for the PMs working with grounded cathode to allow grounding of the tube shieldings and an A.C. coupled preamp which drives the cables carrying the signals outside of the magnet yoke. The signals enter three way splitters, providing input to a constant fraction discriminator, a driver for amplitude measurements and first level analog sums for trigger generation. All these functions are mounted on a 9U VME card, containing 30 complete channels. Signals from this card go to the KLOE designed 12 bit ADC's, 2 V×10 ns full scale, and 12 bit TDC's, 25 ps per count. A description of KLOE electronics can be found in ref. 14.

7. Conclusions

Module Ø was exposed to a test beam at PSI this past July. Analysis of the collected data is underway at present, preliminary results indicate that $\sigma_E/E \sim 5\%/\sqrt{E\ (\mathrm{GeV})}$ and $\sigma_T \sim 66\mathrm{ps}/\sqrt{E\ (\mathrm{GeV})}$. These results are precisely the expected resolutions taking into account the length of the full module (4.3 m) and the reduced quantum efficiency of the mesh PM's, halving the number of photoelectrons.

In sum, we have studied extensively the performance of both the *barrel* and *end-cap* prototypes of the KLOE calorimeter and confirmed the findings with module Ø. Aside from the measured energy and time resolutions quoted, we found the energy resolution to be independent of the incidence angle and we expect very little dependence of the time resolution on incidence. We have verified that the calorimeter can provide some added means to identify pions and muons. Finally, the KLOE electronics performed extremely well at the PSI test, fully to specifications and with very low noise. Therefore, we have succeeded in the design of a calorimeter which satisfy, with some safety margins the requirements of the KLOE experiment.

ACKNOWLEDGEMENTS

We thank W. Kluge and his group, the PSI management and technical staff for their hospitality, help and support during our work at PSI, thank the LADON group for their help and collaboration. We acknowledge the efforts of the SPECAS mechanical shop for the construction of the prototypes. We also thank A. Balla and G. Corradi and M. Santoni for help with the electronics, and especially M. Anelli and A. Rutili for their help in setting up and testing the calorimeter.

REFERENCES

1. The KLOE Coll. *KLOE, A General Purpose Detector*, LNF-92/019 (1992).
2. G. Vignola, *Proc. of the XXVI Int. Conf. on HEP*, ed. J. Sanford AIP (1992) 1941.
3. The KLOE Coll. *The KLOE Detector Technical Proposal*, LNF-93/002 (1993).
4. G. de Zorzi, *Proc. of 4th Int. Conf. on Calorimetry*, La Biodola, Italy (1993).
5. H. Hinterberger, R. Winston, Rev. Sci. Instr. 37 (1966) 1094; A. Di Domenico *et al.*, KLOE Notes 83 and 84.
6. S. Miscetti, *Proc. of 4th Int. Conf. on Calorimetry*, La Biodola, Italy (1993).
7. J. Lee-Franzini, *Proc. of 6th Int. Conf. on Advanced Detectors*, Elba, PISA, Italy (1994).
8. D. Babusci *et al.*, Nucl. Instr. and Meth. 305 (1991) 19.
9. S. Miscetti and A. Parri, KLOE note 111 (1994).
10. The KLOE Coll. *The KLOE Central Drift Chamber*, LNF-94/028 (1994).
11. C. Bini *et al.*, KLOE Notes 42, 50, 60, and 78; G. Barbiellini *et al.*, KLOE Notes 56 and 81.
12. F. Bossi, KLOE notes 54 and 91.
13. L. Keeble, G. Lanfranchi and M. Anelli, KLOE Notes 90, 96 and 109.
14. The KLOE Coll. *The KLOE Data Acquisition System*, LNF-94, (1994).